Colloids and Surfaces A: Physicochem. Eng. Aspects 384 (2011) 145–149

Contents lists available at ScienceDirect

Colloids and Surfaces A: Physicochemical and Engineering Aspects

journal homepage: www.elsevier.com/locate/colsurfa

# Comparative oxidation of adsorbed asphaltenes onto transition metal oxide nanoparticles

Nashaat N. Nassar*, Azfar Hassan, Pedro Pereira-Almao*

*Alberta Ingenuity Centre for In-Situ Energy, Department of Chemical and Petroleum Engineering, University of Calgary, Calgary, Alberta, Canada*

ARTICLE INFO

*Article history:*
Received 7 February 2011
Received in revised form 13 March 2011
Accepted 24 March 2011
Available online 2 April 2011

*Keywords:*
Nanoparticles
Asphaltenes
Oxidation
Adsorption
Activation energy
Metal oxide

ABSTRACT

In this study asphaltenes – waste hydrocarbons and problematic constituent present in heavy oil – have been investigated for its oxidation onto different types of nanoparticles, namely NiO, $Co_3O_4$ and $Fe_3O_4$. All nanoparticles tested showed high adsorption affinity and catalytic activity for asphaltene adsorption and oxidation in the following order NiO > $Co_3O_4$ > $Fe_3O_4$. The oxidation temperature of asphaltenes decreased by 140, 136 and 100 °C with respect to non-catalytic oxidation in the presence of NiO, $Co_3O_4$, and $Fe_3O_4$ nanoparticles, respectively. A correlation appears to exist between the adsorption affinity and the catalytic activity, the higher the affinity the greater the catalytic activity.



## 1. Introduction

As the world demand for the conventional crude oil is growing and the decline in this conventional crude oil is expected in coming future, Alberta oilsands have now become an important source of fossil fuel. Actually, the International Energy Agency (IEA) has predicted that, by the year 2030, about 60% of the total worldwide energy growth will be met by fossil fuel sources such as heavy oil, coal, and natural gas [1]. Nonetheless, due to its high viscosity, low hydrogen to carbon ratio and high sulphur and nitrogen content, oilsands production faces several challenges that need to be surmounted to make it a sustainable and economically feasible alternative [2–6]. Among the challenges to be solved are the reduction in costs associated with the production and transportation of oilsands and the improvement of synthetic crude quality to meet stringent market specifications with less environmental footprints. Nanotechnology is a rapidly growing technology with considerable potential applications and benefits [7–10]. Recently, nanoparticles have attracted interest for their unique properties in various fields in comparison to their bulk counterparts. Nanoparticles can be used to sustain oilsands industry through the development of greener processes with cost-effective approach. Among the numerous application of nanotechnology for energy and the environment, adsorption and oxidation of asphaltenes – waste hydrocarbons and problematic constituent present in heavy oil – on nanoparticle surfaces is one of the most recent examples [11–13]. Asphaltenes are aromatic macromolecules containing heteroatoms present in heavy oil matrix that make heavy oil difficult to upgrade and process. Removal of asphaltenes from crude oil has therefore great significance. This work looks at in situ heavy oil upgrading by the removal of asphaltenes with nanoparticles, followed by catalytic oxidation or steam gasification. By integrating heavy oil deasphalting technique with that of oxidation, important synergies would be realized. These include reduction in capital cost, increase in energy efficiency, and enhanced performance and portability [14]. In the present study, the catalytic effect of different nanoparticles (NiO, $Co_3O_4$ and $Fe_3O_4$) towards asphaltenes oxidation is investigated. A correlation between the adsorption affinity and the catalytic activity of nanoparticles towards asphaltene adsorption and oxidation is reported for the first time. Catalytic steam gasification of asphaltenes in the presence of nanoparticles has been addressed in our previous study [15].

## 2. Experimental and methods

### 2.1. Nanoparticles

Three types of transition metal oxide nanoparticles, namely NiO, $Co_3O_4$ and $Fe_3O_4$ were used in this study. NiO and $Co_3O_4$ were purchased from Sigma–Aldrich, ON; while $Fe_3O_4$ was obtained from Nanostructured & Amorphous Materials, Inc., TX, USA. Par-

* Corresponding authors.
*E-mail addresses:* nassar@ucalgary.ca (N.N. Nassar), ppereira@ucalgary.ca (P. Pereira-Almao).

0927-7757/$ – see front matter © 2011 Elsevier B.V. All rights reserved.
doi:10.1016/j.colsurfa.2011.03.049

**Table 1**
Particle size and surface areas of selected transition metal oxide nanoparticles.

| Nanoparticles | Particle size (nm)[a] | Specific surface area, BET ($m^2/g$) | External surface area, *t*-plot ($m^2/g$) |
|---|---|---|---|
| $Co_3O_4$ | 22 ± 0.8 | 41 | 39 |
| $Fe_3O_4$ | 22 ± 1.5 | 43 | 37 |
| NiO | 12 ± 2.3 | 107 | 94 |

[a] Determined by X-ray diffraction.

ticle size, BET and external surface areas are presented in Table 1. Particle size was determined by using X-ray Ultima III Multi Purpose Diffraction System (Rigaku Corp., The Woodlands, TX) with Cu Kα radiation operating at 40 kV and 44 mA with a $\theta$–$2\theta$ goniometer. Surface areas of the nanoparticles were measured by a surface area and porosity analyzer (TriStar II 3020, Micromeritics Corporate, Norcross, GA). Surface area was measured by performing $N_2$-adsorption–desorption at 77 K. The samples were degassed at 150 °C under $N_2$ flow overnight before analysis. Surface areas were calculated using Brunauer–Emmet–Teller (BET) equation. External surface areas were obtained by *t*-plot method and there was no significant difference between the surface areas obtained by BET and *t*-plot methods, suggesting that the nanoparticles are non-porous.

### 2.2. Asphaltenes and solvents

Asphaltenes were extracted from a vacuum residue sample originally obtained from Athabasca bitumen in Alberta. Solvents used in the precipitation and extraction were *n*-heptane (99% HPLC grade, Sigma–Aldrich, ON), *n*-pentane (99% HPLC grade, Sigma–Aldrich, ON) and toluene (analytical grade, EMD, MERCK, NJ). Asphaltene extraction followed a similar procedure employed in our previous study [11]. Briefly, a specified amount of vacuum residue was mixed with *n*-heptane at a ratio of 1:40 (g/mL). The mixture was then sonicated in a water bath at 25 °C for 2 h and left shaking at 300 rpm for one day to equilibrate. Black precipitated asphaltenes settled at the bottom and then were collected after decanting the supernatant. Then, the precipitated asphaltenes were washed with fresh *n*-heptane at a ratio of 1:4 (g/mL) and centrifuged at 5000 rpm for 5 min and left to stand overnight. The asphaltenes were separated from the final solution by filtration using an 8-μm Whatman filter paper. The resultant asphaltenes washed thoroughly with *n*-heptane, homogenized and fined using a pestle and mortar. After that the asphaltenes were left to dry at room temperature in a hood until no change in mass was observed.

### 2.3. Heavy oil model solutions

The heavy oil model solutions were prepared by re-dissolving the prepared asphaltenes in toluene at a specified concentration. All samples were prepared from a stock solution containing 4000 mg/L asphaltenes diluted to different concentrations by addition of toluene.

### 2.4. Batch adsorption experiments

Adsorption of asphaltenes onto the selected different nanoparticles was performed at 25 °C, as described in our previous study [11]. Briefly, batch adsorption experiments were carried out by adding 100 mg of nanoparticles to a 10-mL of asphaltenes–toluene solution. The mixture was shaken at 200 rpm in an incubator at 25 °C for 24 h, as it was adequate time to achieve equilibrium [11,12]. Then, the nanoparticle-containing asphaltenes were separated via centrifugation at 5000 rpm for 30 min. The supernatant was decanted and the precipitate, i.e., nanoparticles containing adsorbed asphaltenes, was placed in vacuum oven at 60 °C for 24 h to evaporate any remaining toluene. Then the sample was subjected to thermal analysis for estimating the adsorbed amount of asphaltenes and oxidation study.

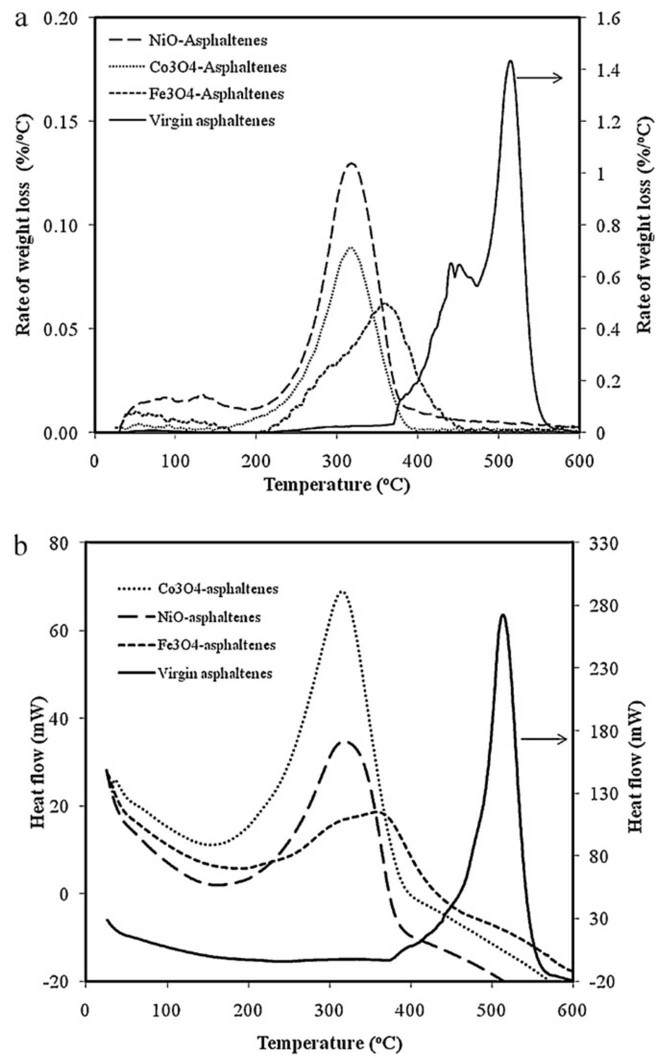


**Fig. 1.** TG–DTA curves for asphaltenes with and without nanoparticles. (a) Plot of rate of mass loss as a function of temperature and (b) plot of enthalpy changes as a function of temperature, heating rate = 10 °C/min; air flow, 100 $cm^3$/min.

#### 2.4.1. Thermogravimetric analysis of asphaltenes

Thermogravimetric analysis was carried out by TGA/DSC analyzer (SDT Q600, TA Instruments, Inc., New Castle, DE) between 200 and 600 °C. Sample mass was kept low to avoid diffusion limitations. The flow rate of air was maintained at 100 $cm^3$/min throughout the experiment. Fresh nanoparticles from the original bottle were heated up to 1000 °C to get a complete profile of mass loss and heat changes.

## 3. Results and discussions

### 3.1. Asphaltene oxidation

Thermal analysis was performed in order to get more insight about the catalytic effect of nanoparticles on asphaltene oxidation. By performing simultaneous thermal analysis both mass and heat changes with time can be monitored. Fig. 1a and b shows the profiles for rate of mass loss and heat changes, respectively, with the increase in temperature under air atmosphere for vir-

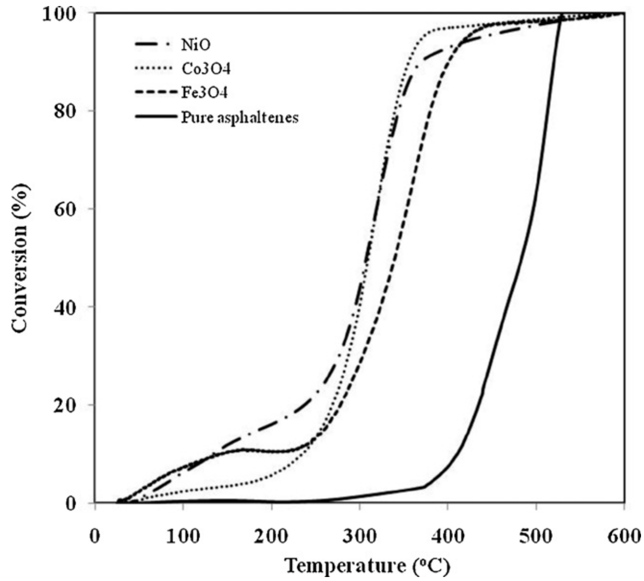


**Fig. 2.** Effect of different types of nanoparticles on % conversion of asphaltenes.

gin asphaltenes and different nanoparticles containing adsorbed asphaltenes.

For virgin asphaltene oxidation, the mass loss profile was divided into two regions, namely low temperature range up to 400 °C and high temperature range beyond 400 °C. As asphaltenes are heavy fractions of oil, no significant mass change can be observed before 400 °C. As seen in Fig. 1a, the mass loss of virgin asphaltenes occurs in two steps, between 400 and 450 °C due to thermal cracking with low temperature oxidation and beyond 450 °C due to complete oxidation to gaseous products. Because there is no exothermicity associated with mass loss up to 450 °C in the profile of heat changes (Fig. 1b), this mass loss was termed as low temperature oxidation region where the major loss occurs due to bond scission as well as incorporation of oxygen into the asphaltene matrix. Oxidation in presence of air occurs after 450 °C as evidenced by the presence of an exotherm that follows the same profile as the mass loss. For the nanoparticles containing asphaltenes, the profile of mass loss as well as heat evolved changed drastically. When adsorbed onto nanoparticles combustion/oxidation of asphaltenes occurs at a much lower temperatures (325–365 °C). NiO and $Co_3O_4$ nanoparticles decrease the oxidation temperature to around 325 °C while asphaltenes oxidation in the presence of $Fe_3O_4$ nanoparticles occurs around 365 °C. This decrease in combustion/oxidation temperature validates the idea that these nanoparticles catalyze the oxidation of asphaltenes considerably with NiO and $Co_3O_4$ being more active than $Fe_3O_4$. Fig. 2 shows a plot of % conversion ratio or the extent of the oxidation reaction, $\alpha$, of asphaltenes with and without nanoparticles as a function of temperature. Where $\alpha$ was estimated as per Eq. (1):

$$\alpha = \frac{w_0 - w_t}{w_0 - w_\infty} \tag{1}$$

where $w_0$ is the initial sample mass, $w_\infty$ is the final sample mass and $w_t$ is the sample mass at any time.It appears that in the absence of nanoparticles, thermal decomposition (pyrolysis) started beyond 350 °C and reached a maximum rate at around 475 °C, showing occurrence of combustion reaction during oxidation. It is evident from the figure that the presence of nanoparticles greatly enhances the oxidation process; as the reaction started as early as 150 °C. This decrease in oxidation temperature shows the catalytic behavior of nanoparticles on oxidation of asphaltenes. These nanoparticles behave differently in low temperature range; however activity for NiO and $Co_3O_4$ becomes almost the same with increase in temperature, which could be attributed to the low amount of asphaltenes remaining over nanoparticles. Catalytic effect of $Fe_3O_4$ stayed different throughout. Interestingly, although NiO has the highest surface area, while surface areas of Co3O4 and Fe3O4 are similar, the catalytic activity of NiO in terms of percent conversion resembled that of Co3O4. This suggests that the surface area is not the only controlling parameter for the catalytic activity. Apparently, the interactions between asphaltenes–nanoparticles are also important and play a role in catalytic activity, as will be discussed in details in the following section.

### 3.2. Estimation of activation energies

Activation energy was calculated by processing simultaneous thermal analysis data following the Coats–Redfern method [16]. Detail description of this method can be found elsewhere [16]. For a reaction mechanism of $f(\alpha)=(1-\alpha)^n$, where $n$ is the order of the reaction, Coats–Redfern stated that:

$$\frac{AR}{\beta E_a}\left(1 - \frac{2RT}{E_a}\right)\exp\frac{-E_a}{RT} = \begin{cases} \ln\left(\frac{-\ln(1-\alpha)}{T^2}\right), & n = 1 \\ \ln\left(\frac{1-(1-\alpha)^n}{(1-\alpha)T^2}\right), & n > 1 \end{cases} \tag{2}$$

where $A$ is the pre-exponential factor (1/s), $E_a$ is the activation energy (KJ/mol) and $R$ is the ideal gas constant (8.314 J/mol K), $T$ is the reaction temperature in K, and $\beta = dT/dt$. If $n$ is known, then a plot of right-hand-side of Eq. (2) versus $1/T$ would give a straight line with slope = $E_a/R$. Accordingly, the activation energies for the overall reaction were obtained from the slopes of $\ln((-\ln(1-\alpha))/T^2)$ versus $1/T$. Table 2 shows the activation energy values for oxidation of virgin asphaltenes and for its oxidation after adsorption over different nanoparticles. It is worth noting that, for virgin asphaltenes, the activation energy was calculated for three distinct temperature regions between 225 and 515 °C. As shown in

**Table 2**
Calculated activation energies for asphaltenes in the presence and absence of nanoparticles at different temperatures.

| | | 227–372 °C | 372–467 °C | 467–514 °C |
|---|---|---|---|---|
| Virgin asphaltenes | $E_a$ (kJ/mol) | 42 | 108 | 91 |
| | $R^2$ | 0.982 | 0.999 | 0.980 |
| | | 280–350 °C | ≥350 °C | |
| Asphaltenes adsorbed onto nanoparticles | | | | |
| NiO | $E_a$ (kJ/mol) | 57 | 0.0 | 0.0 |
| | $R^2$ | 0.997 | | |
| $Co_3O_4$ | $E_a$ (kJ/mol) | 72 | 0.0 | 0.0 |
| | $R^2$ | 0.999 | | |
| $Fe_3O_4$ | $E_a$ (kJ/mol) | 43 | 61 | 0.0 |
| | $R^2$ | 0.997 | 0.999 | |

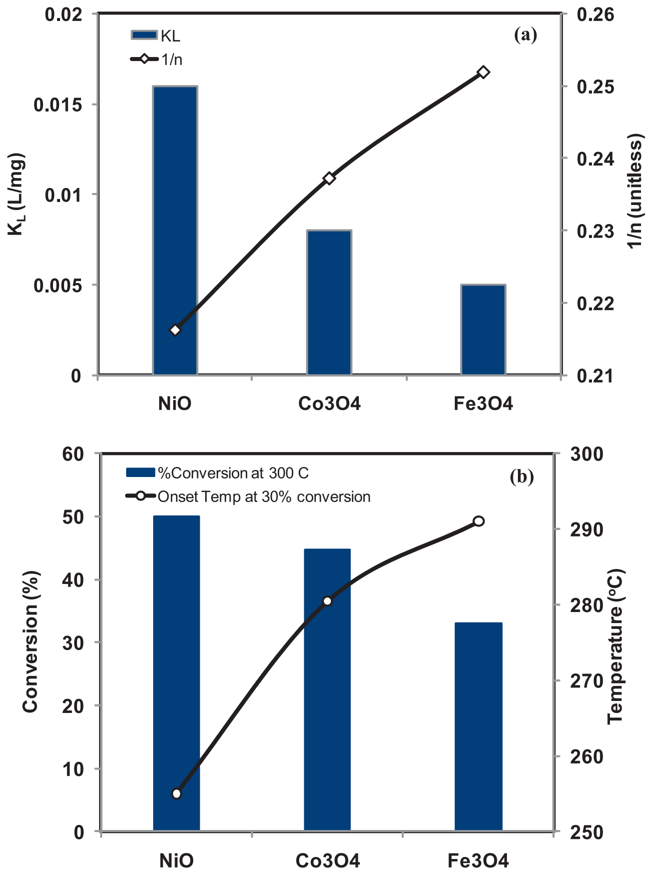


**Fig. 3.** Relationship between adsorption affinity and catalytic activity of different nanoparticles: (a) Langmuir and Freundlich adsorption affinity constants ($K_L$ and $1/n$, respectively) obtained from reference [11] and (b) % conversion and oxidation temperature of asphaltenes in the presence of nanoparticles.

Table 2 the activation energy values determined for the oxidation of asphaltenes when adsorbed over nanoparticles decreased with significant decrease in the oxidation temperature. When adsorbed over NiO and $Co_3O_4$ nanoparticles, asphaltenes were completely oxidized before 350 °C. In case of $Fe_3O_4$, oxidation reaction was not very rapid and as a consequence activation energies are listed in two temperature regions. From the above mentioned results, it is evident that the presence of nanoparticles caused a drop in the oxidation temperature, hence showing their catalytic effect.

### 3.3. *Relationship between adsorption affinity and catalytic activity of nanoparticles*

Clearly, nanoparticles have shown strong affinity and catalytic activity towards asphaltene adsorption and oxidation. One interesting correlation found to exist was the relationship between adsorption affinity constant and the catalytic activity as shown in Fig. 3a and b, respectively. Fig. 3a shows the values obtained for affinity constants calculated for the three nanoparticles in our previous study using Langmuir and Freundlich adsorption models [11]. The affinity constant was highest for NiO and lowest for $Fe_3O_4$. Affinity constant is a measure of the interaction between adsorbate and adsorbent. The higher the value, the greater the strength of interaction. Fig. 3b shows the values of catalytic activity in terms of percent conversion at a given temperature and also in terms of onset temperature at a given percent conversion (30%). Again, NiO shows highest percent conversion at a given temperature probably because the adsorbate–adsorbent interactions are the strongest. On the other hand, $Fe_3O_4$ with lowest adsorption

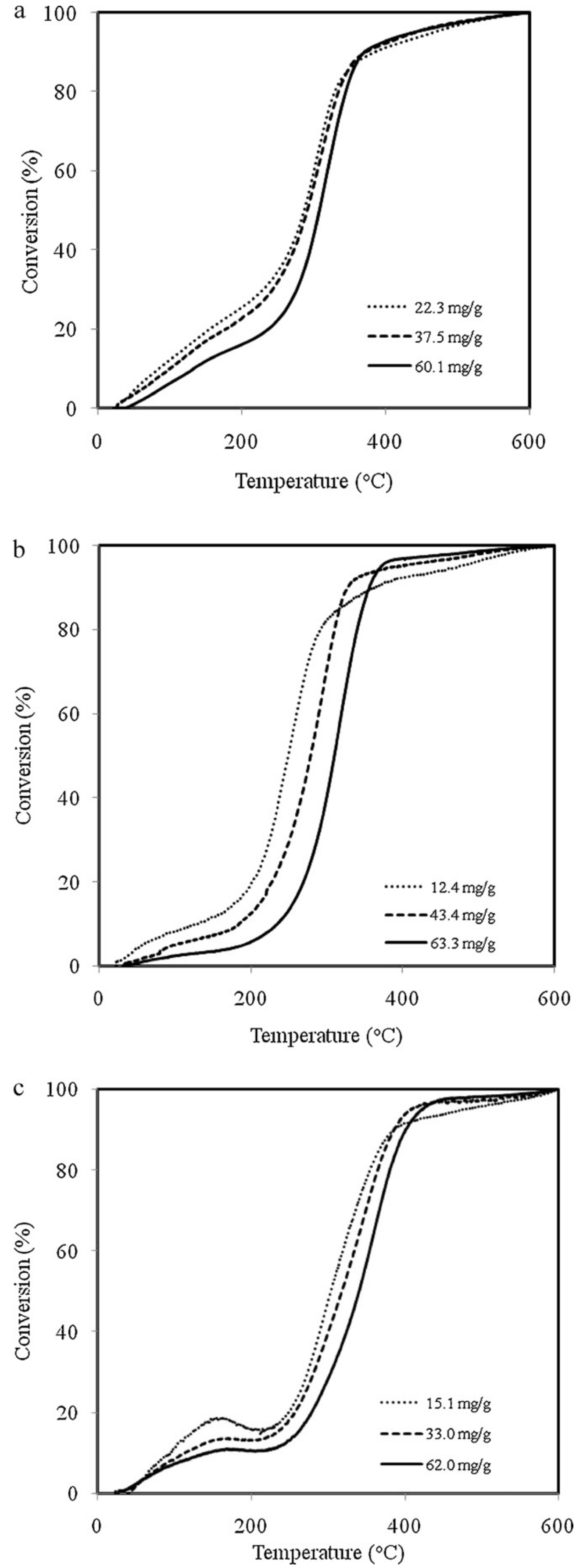


**Fig. 4.** Effect of the adsorbed amount of asphaltenes on the catalytic activity of metal oxide nanoparticles, (a) NiO, (b) $Co_3O_4$ and (c) $Fe_3O_4$.

**Table 3**
Adsorbed amount of asphaltenes onto different surfaces of nanoparticles at 25 °C.

| Nanoparticles | Asphaltene initial concentration (mg/L) | Adsorbed amount of asphaltenes (mg/g) |
|---|---|---|
| NiO | 200 | 22.3 |
| | 500 | 37.5 |
| | 2000 | 60.1 |
| $Co_3O_4$ | 200 | 12.4 |
| | 500 | 43.4 |
| | 2000 | 63.3 |
| $Fe_3O_4$ | 200 | 15.1 |
| | 500 | 33.0 |
| | 2000 | 62.0 |

affinity shows the lowest catalytic activity. A comparison of Figs. 3a and b shows that the catalytic activity is directly related to affinity constant.

### 3.4. Effect of asphaltene loading on the catalytic activity of nanoparticles

In practice, asphaltene oxidation and % conversion will be dependent on the asphaltene loading. In this set of experiments, metal oxide nanoparticle containing different adsorbed amount of asphaltenes were oxidized using TGA. It can be seen in Table 3 that increasing the initial concentration of asphaltenes increases the adsorbed amount of asphaltenes onto nanoparticles. Oxidations were performed to study the effect of asphaltene loading on the catalytic activity of nanoparticles. Fig. 4a–c shows that, for all the selected nanoparticles, asphaltene oxidation is enhanced as the adsorbed amount of asphaltenes decreased. As the amount of nanoparticles is fixed, an increase in the adsorbed amount of asphaltenes results in the accumulation of asphaltene molecules onto nanoparticle surfaces and hence reduces the active sites available for reaction.

## 4. Conclusions

In this work, nanoparticles of $Co_3O_4$, $Fe_3O_4$ and NiO were employed for the adsorptive removal of asphaltenes from heavy oil model solution followed by asphaltene oxidation. All nanoparticles tested in this study showed high adsorption affinity towards asphaltenes in the following order NiO > $Co_3O_4$ > $Fe_3O_4$. The nanoparticles tested showed high catalytic activity for asphaltenes oxidation in the same order. This suggests that a correlation appears to exist between the affinity constant and the catalytic activity, the higher the affinity constant the greater the catalytic activity. As expected, the catalytic activity of all selected nanoparticles decreased as the adsorbed amount of asphaltenes onto nanoparticles increased.

## Acknowledgement

The authors acknowledge the financial support provided by Carbon Management Canada Inc. (CMC).

## Appendix A. Supplementary data

Supplementary data associated with this article can be found, in the online version, at doi:10.1016/j.colsurfa.2011.03.049.

## References

[1] K. Kobayashi, Forecasting Supply and Demand up to 2030, International Energy Agency, 2005.
[2] P. Pereira, T. Romero, J. Velasquez, A. Tusa, I. Rojas, W. Camejo, M. IRosa-Brussin, Combined steam conversion process for treating vacuum gas oil. United States Patent 6,030,522 (2000).
[3] P. Pereira, R. Marzin, L. Zacarias, J. Cordova, J. Carrazza, M. Marino, Steam conversion process and catalyst. United States Patent 5,885,441 (1999).
[4] J. Carrazza, P. Pereira, N. Martinez, Process and catalyst for upgrading heavy hydrocarbon. United States Patent 5,688,741 (1997).
[5] C.E. Galarraga, P. Pereira-Almao, Hydrocracking of athabasca bitumen using submicronic multimetallic catalysts at near in-reservoir conditions, Energy Fuels 24 (2010) 2383–2389.
[6] C. Sosa-Stull, G. Trujillo-Ferrer, F. Lopez-Linares, P. Pereira-Almao, Athabasca Bitumen Upgrading Using Different Species of the Same Ultra Dispersed Catalyst Formulation, American Chemical Society, San Francisco, CA, USA, 2010.
[7] L. Patruyo, Removal of $H_2S$(g) Using Ultradispersed Iron Oxide Nanoparticles in, Department of Chemical and Petroleum Engineering, University of Calgary, Calgary, 2008.
[8] M.M. Husein, N.N. Nassar, Nanoparticle preparation using the single microemulsions scheme, Curr. Nanosci. 4 (2008) 370–380.
[9] M.M. Husein, L. Patruyo, P. Pereira-Almao, N.N. Nassar, Scavenging $H_2S$(g) from oil phases by means of ultradispersed sorbents, J. Colloid Interface Sci. 342 (2010) 253–260.
[10] N.N. Nassar, M.M. Husein, P. Pereira-Almao, Ultradispersed particles in heavy oil: Part II, sorption of $H_2S$(g), Fuel Process. Technol. 91 (2010) 169–174.
[11] N.N. Nassar, A. Hassan, P. Pereira-Almao, Metal oxide nanoparticles for asphaltene adsorption and oxidation, Energy Fuels 25 (2011) 1017–1023.
[12] N.N. Nassar, Asphaltene adsorption onto alumina nanoparticles: kinetics and thermodynamic studies, Energy Fuels 24 (2010) 4116–4122.
[13] D. Dudášová, S. Simon, P.V. Hemmingsen, J. Sjöblom, Study of asphaltenes adsorption onto different minerals and clays: Part 1. Experimental adsorption with UV depletion detection, Colloids Surf. A: Physicochem. Eng. Aspects 317 (2008) 1–9.
[14] P.S. Wallace, M.K. Anderson, A.I. Rodarte, W.E. Preston, Heavy oil upgrading by the separation and gasification of asphaltenes, in: Gasification Technologies Conference, San Francisco, CA, 1998.
[15] N.N. Nassar, A. Hassan, P. Pereira-Almao, Application of nanotechnology for heavy oil upgrading: Catalytic steam gasification/cracking of asphaltenes, Energy Fuels (2011) in press.
[16] A.W. Coats, J.P. Redfern, Kinetic parameters from thermogravimetric data, Nature (1964) 68–69.